WORLD JOURNAL OF PHARMACEUTICAL RESEARCH
SJIF Impact Factor 5.990
Volume 4, Issue 12, 1126-1138. Research Article ISSN 2277– 7105

SPECTRAL, ELECTROCHEMICAL AND MOLECULAR MODELING STUDIES OF SULFASALAZINE

Dr.Vijay Bhaskar and A Ramachandraiah*

Department of Chemistry, National Institute of Technology Warangal, Warangal, 506004, Andhra Pradesh, India.

Article Received on
02 Oct 2015,

Revised on 23 Oct 2015,
Accepted on 12 Nov 2015

***Correspondence for Author**
Dr.Vijay Bhaskar
Department of Chemistry, National Institute of Technology Warangal, Warangal, 506004, Andhra Pradesh, India.

ABSTRACT

The spectral and voltammetric behavior of sulfasalazine (**1H$_2$**) in aqueous buffers of varied pH is presented. Spectrophotometry and cyclic voltammetry were utilized to study its proton and electron transfer characteristics respectively. Relevant thermodynamic and electrochemical data such as deprotonation constant (pK_a), charge transfer co-efficient (α_{na}), forward rate constant ($k^0_{f,h}$), etc, have been evaluated. An excellent electroanalytical assaying of **1H$_2$** has been developed in differential pulse polarography at *p*H = 8. Molecular modeling on various acid-base conjugates of **1H$_2$** and their several conformers has been carried out to arrive at the thermodynamic and conformational issues to correlate to the spectral and electrochemical observations.

KEYWORDS: Sulfasalazine, acid-base equilibria, cyclic voltammetry, molecular modeling, conformational energy plots, isosbestic points.

INTRODUCTION

Azo compounds are the largest class of industrial organic dyes. Despite the fact that many azo compounds are toxic, dozens of other monoazo dyes are permitted in drugs and cosmetics. The pharmaceutical importance of alkyl and aryl azo compounds has been extensively reported.[1] The redox behaviour of these compounds plays an important role in their biological activity.[2] More than 50% of commercially used azo dyes contain a naphthol ring and thereby exhibit a naphthone-naphthol tautomerism.[4]

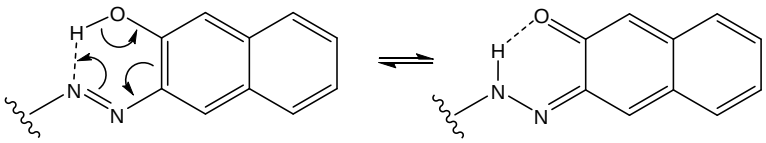

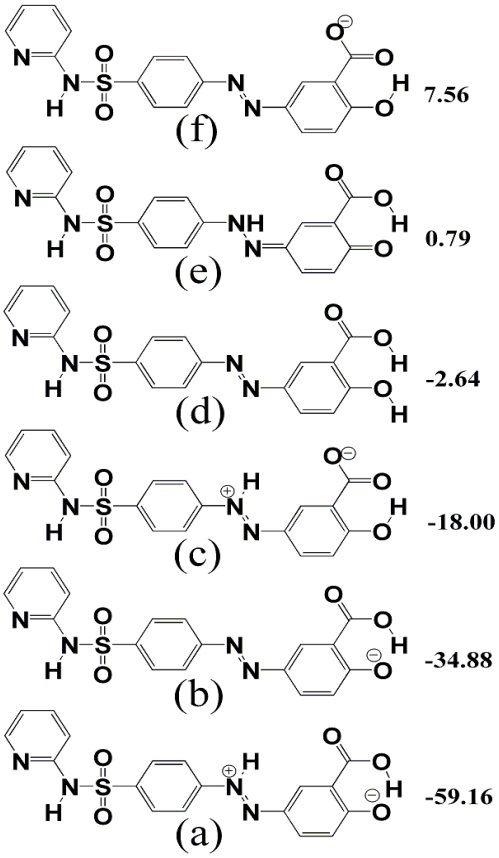

1H$_2$

Naturally, the naphthol tautomer is more populated in acidic buffers whereas the naphthone in alkaline media. Hence, azo compounds with naphthol and phenol group at vantage positions promise highly pH-dependent spectral and electrochemical properties. The voltammetric behaviour of the synthesized azo compounds has been extensively reported in the literature.[3,5-8]

Sulfasalazine, shown in different possible tautomeric forms in **1H$_2$**, is a potential antibiotic drug. It is commonly known as salicylazosulfapyridine or salazosulfapyridine. Despite its pharmaceutical, photochemical and dying characteristics, no noteworthy electrochemical investigations of **1H$_2$** are found in literature. We present here detailed acid-base, electrochemical and preliminary molecular modeling studies of this important colourful drug. Some of the physical, analytical, spectral and relevant data of **1H$_2$** are collected in **Table 1**. In structure **1H$_2$** are also shown the heats of formation of the various tautomeric forms of **1H$_2$**.

In fact, **$1H_2$ (e)** is shown as the structure of **$1H_2$** in Wikipedia though gas phase molecular modeling studies of **$1H_2$** are in favour of other Zwitter ions, **$1H_2$ (a), $1H_2$ (b)** and **$1H_2$ (c)**.

Experimental

All the chemicals used were of AnalaR grade. Several tablets of Sulfasalazine were crushed and leached into warm water and then the drug was regenerated by a slow addition of $NaHCO_3$ solution. The azo drug was then recrystallized from ethanol. A milli molar stock solution of **$1H_2$** was prepared in ethanol. Every time before the spectral or electrochemical run, 1 ml of the stock solution was placed in a 25 ml standard flask and was made up by the buffer of the desired pH (ionic strength = 0.02 M).[9] The corresponding blank solution was similarly made by just making up 1 ml of ethanol. An ATI Orion Model 902 Ion Meter was used for the pH-metry whereas an AnalyticJena Specord 205 Ratio Recording Spectrophotometer for uv-vis spectral and a Metrohm 663 VA Stand for voltammetric (on mostly an SMDE) and a BAS CV-27 Voltammograph for coulometric studies. Molecular modeling was carried out on a Chem Office Ultra Pro 10.0 platform.

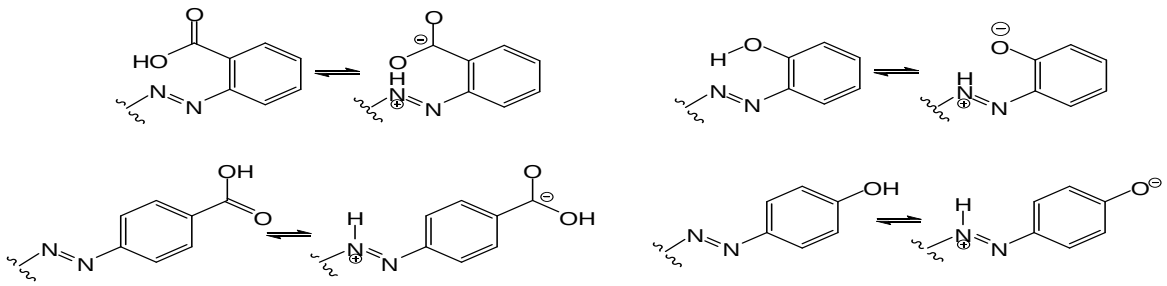

RESULTS AND DISCUSSION

Spectral Studies and Acid-Base Equilibria Sulfasalazine, **$1H_2$**, has two acidic moieties in phenol and carboxylic groups while similar number of basic sites in pyridine and the azo groups. The salicylic acid moiety, known for its classical case of intramolecular hydrogen bonding, present in **$1H_2$**, would render both the phenolic and the carboxylic protons less acidic. Further, the two deprotonation constants are expected to be considerably different because the carboxylate also stabilizes phenolic group by intramolecular hydrogen bonding. It is also reported that azo benzenes with either ortho or para labile protic groups such as carboxylic acid or phenolic groups exhibit tautomerisim to offer a zwitter ion in aqueous media as at pHs close to the pK_a of the said acid group.[3] In the case of **$1H_2$**, however, we have the carboxylic group in a meta position whereas the phenolic is in para position to the azo group. The expected proton transfer equilibria of **$1H_2$** along with some possible

tautomerism and resonance are presented in **Scheme 1**. As many as four pK_a values are expected for $\mathbf{1H_4^{2+}}$, the doubly protonated $\mathbf{1H_2}$, as proposed in **Scheme 1** on the basis of the structure of $\mathbf{1H_2}$ and the known acid-base chemistry salicylic acid and of pyridine phenolic and azophenolic groups. The electronic spectra of $\mathbf{1H_2}$ in aqueous buffers of pH range, 3-11, are shown in **Figure 1**. From the bonding scheme of $\mathbf{1H_2}$ and its tautomeric zwitters, $\mathbf{1H_2(carb)}$

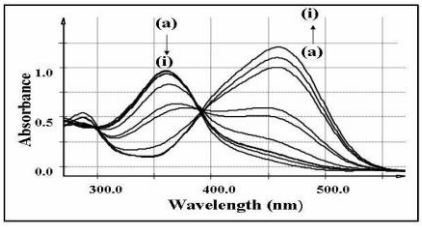

Figure 1: *UV-Visible spectra of* ***1H₂*** (1.05x10^{-4} M) *at pH (a) 3.62, (b) 4.54, (c) 6.05, (d) 8.57, (e) 9.01, (f) 9.31, (g) 9.73, (h) 10.21, (i) 10.75*

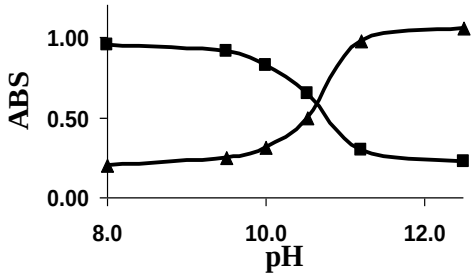

Figure 2: *Variation of absorbance with pH of* ***1H₂*** *at (-■-) 359 nm and (-▲-) 469 nm. The thick lines are curve-fit for* pK_a *of 10.83*

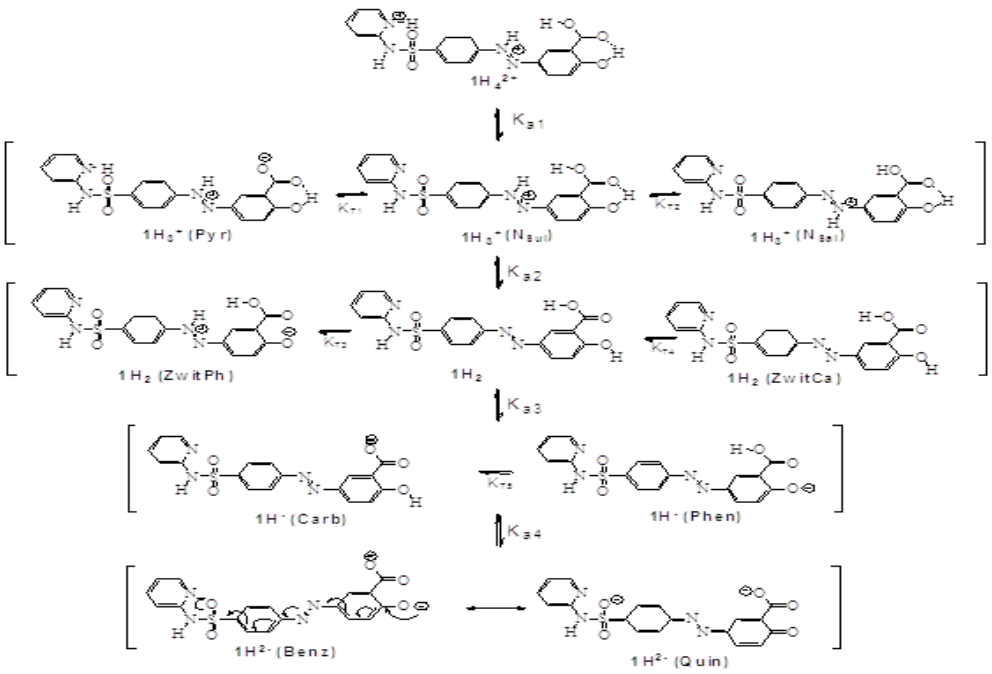

Scheme 1

and **$1H_2$(phen)**, in all of which the π system is same, one may not expect any spectral variation in low pH region because the proton shift and the protonation of basic nitrogens would hardly influence the $\pi \rightarrow \pi^*$ transitions of the salicylic acid or the azo groups or the pyridine ring because the lone pairs are orthogonal to the π skeleton and the acid groups are exocyclic. Similarly, the acid-base equilibrium between **$1H_2$** and **$1H^-$** may also not be associated with any spectral variation. However, one may expect a great deal of spectral variation once the phenolic proton is removed, i.e., in the conversion of **$1H^-$** into **1^{2-}** because it is accompanied by a resonance between azophenoxide and phenone-hydrazone moieties. The overlapped electronic spectra of **$1H_2$** in buffers of varied pHs, shown in **Figure 1**, are clearly in support this expectation. In the pH range, 2-7, **$1H_2$** exhibits an absorption band at ~ 360 nm. Though no significant change was observed in the spectra of **$1H_2$** in this pH range, considerable extent of bathochromic shift was observed in the spectra, in the pH region, 8-11, with a clear isosbestic point at ~ 390 nm with a new and stronger absorption band at ~ 460 nm. Further, the solution exhibits a visual dark orange colour development in the pH range above 9. Since the presence of isosbestic points means the coexistence of only two absorbing species in isomolar stoichiometric equilibrium, the two species are tentatively assigned as **$1H^-$** and **1^{2-}** to absorb at ~ 360 nm and ~460 nm respectively. It is well known that several acid-base indicators owe their colour change at end-points to the benzenoid to quinonoid

conversion accompanied by a bathochromic shift with rise in pH. On the basis of the plots of absorbance vs pH at the two λ_{max}, 360 and 460 nm, it was possible to obtain the pKa_2 of **$1H_2$** (or pKa_4 of **$1H_4^{2+}$** of **Scheme 1**). The two such plots along with their curve-fits are shown in **Figure 2** while the deprotonation constants are placed in **Table 1**.

Electrochemical Studies

The compound **$1H_2$** exhibits an interesting electron transfer behavior that changes its style and profile with *p*H. The cyclic voltammetric response of **$1H_2$** in various *p*Hs is shown in **Figure 3.** Since the structures of the electroactive species vary with pH, the peak potentials and their dependence on the pH also vary with the ranges of pH**.** Compound, **$1H_2$**, has an –N=N- site as the only reducible moiety in its normal structure. Azo compounds are known for their facile reduction of the azo moiety in aqueous media either consecutively as

$$R-N=N-R \xrightarrow{2e,2H^+} R-NH-NH-R \xrightarrow{2e,2H^+} 2R-NH_2 \qquad (1)$$

or directly as

$$R-N=N-R \xrightarrow{4e,4H^+} 2R-NH_2 \qquad (2)$$

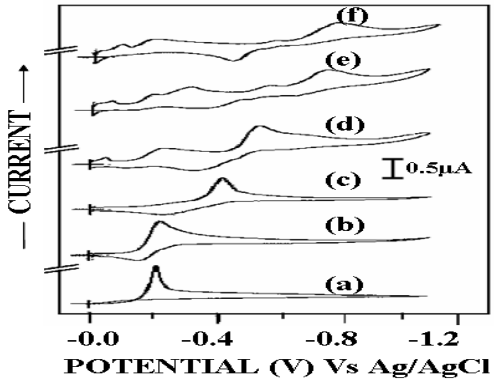

Figure 3: ***Cyclic voltammograms of $1H_2$ (3.5×10^{-5} M) in buffers (ionic strength = 0.05M) of pH (a) 2.56, (b) 4.02, (c) 6.10, (d) 8.65 (e) 10.25, (f) 11.20***

depending on the pH.[10-14] In protic media, azobenzene's reduction occurs in a one-step, two-electron, two-proton reversible reaction.[15] Azo compounds are also known for their adsorptive and non-diffusion-controlled electrochemistry on mercury electrode.[16] However,

in highly acidic media, the -NH-NH- further undergoes electrochemical reductive cleavage to give primary amines.[7]

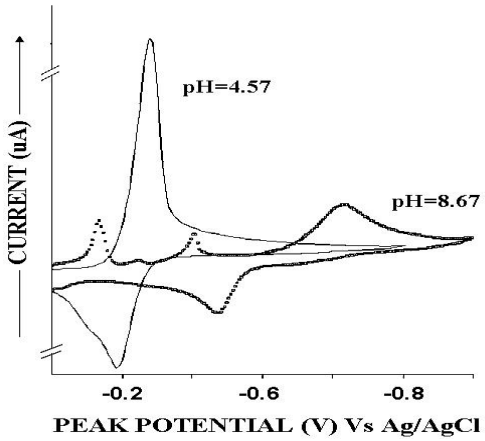

Figure 5: ***Cyclic voltammetric profiles of 1H2 at fast scan rates (1000 mVs^{-1})***

For an electrochemical reduction,

$Ox + ne + mH^+ \rightarrow Red$ (3)

the peak potential, E_p varies with *p*H at 25^0C as

$$E_P = E_P^o - 0.05916\frac{m}{n}pH$$

where E^0_p is the peak potential at reference *p*H. Hence, a plot of E_p vs *p*H should give a straight line, from the slope of which one calculate the number of H^+ ions involved in electrochemical reduction step, provided, one knows the value of n by either coulometry or other means. In **Figure 4** are shown two such plots indicating the effect of pH on the cyclic voltammetric reduction peak potential. The plots of E_p vs *p*H of **$1H_4^{2+}$ and $1H_3^+$** (i.e. in the acid pH range) the slope is compatible to a 4-proton participation while those of **$1H_2$, $1H^-$** and **1^{2-}** to a 2-proton one. Coulometric studies of **$1H_2$** in several buffers gave *n* values as 4 and 2 in acidic and basic pH buffers respectively. With the knowledge of *n* and αn_a, we could evaluate the diffusion coefficient, D, for **$1H_2$** from the Randles-Sevcik equations applicable for an irreversible diffusion controlled and quasireversible adsorptive electron transfer CV steps. The values of D calculated by this method for **$1H_2$** in media of *p*H range 2-12 are also collected in **Table 2**.

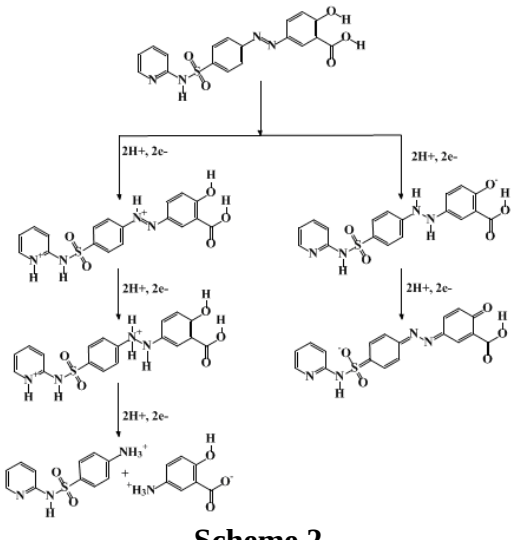

Scheme 2

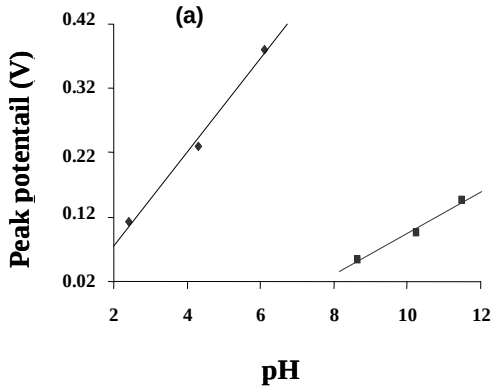

Figure 4: ***Effect of peak potential with pH of 1H₂***

Usually electrochemical reduction of azo group on mercury electrode is adsorptive with only the -N=N- moiety being adsorptive on SMDE but not its reduction product, -NH-NH-. Hence, at slow scan rates, the reduction oxidative peak is usually missing. When the scan rate is enhanced, the reverse anodic potential is quickly reached before the entire –NH-NH- is desorbed and one expects a finite amount of anodic process. In **Figure 5** are shown the effect of scan rate on the cyclic voltammetirc profiles of **1H₂** in both acidic and alkaline media. It can be seen that the irreversible profile at 100 mVs^{1} becomes quasireversible at 1000 mVs^{-1} in the acidic media whereas no such profile variation is observed in the alkaline media. For diffusion controlled and reversible cyclic voltammetirc peaks, the current function, $i_p / v^{1/2}$, where i_p is the peak current and *v*, the scan rate, is independent of scan rate whereas for adsorptive cyclic voltammetirc peaks, the current function, i_p / v, is independent of scan rates.

In the case of **1H$_2$**, we have observed diffusion controlled cv patterns in alkaline media whereas adsorptive electron transfer cv in acidic buffers. The cv profile of **1H$_2$** in alkaline media feature two reduction potentials, one at ~-0.18 V and the other at ~-0.70 V. The lower cathodic but irreversible peak is attributed to a diffusion controlled quinine-hydroquinone type of reduction of the quinonoid species of **1H$_2$** whereas the more cathodic one to the azo group's reductive cleavage from =N-N= to –NH$_2$ and H$_2$N- in a consecutive pair of two-electron-two-proton processes. On the basis of the electrochemical investigations, a plausible electrochemical reduction mechanism of compound **1H$_2$** is presented in **Scheme 2** while various important electrochemical data of **1H$_2$** are collected in **Table 2**.

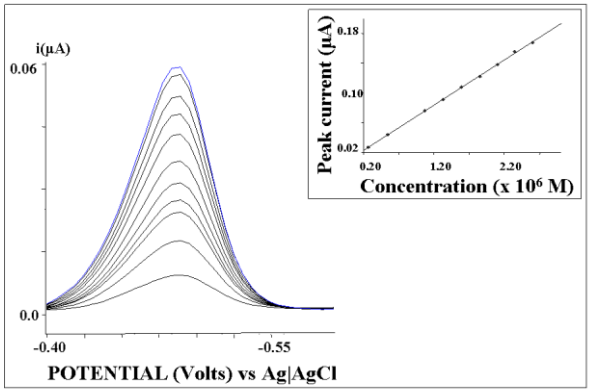

Figure 6*: Differential pulse polarograms of 1H$_2$ from (1 to 8) x10^{-6} M (pulse height =100 mV; SMDE area = 6.25x10^{-6} m^2)*

Assaying of 1H$_2$.

Based on the electrochemical response of **1H$_2$**, an excellent electrochemical assaying of **1H$_2$**, in differential pulse polarography (DPP), is developed. The DPP curves of **1H$_2$** at *p*H=4.00 along with the calibration curve (inset) are shown in **Figure 6.**

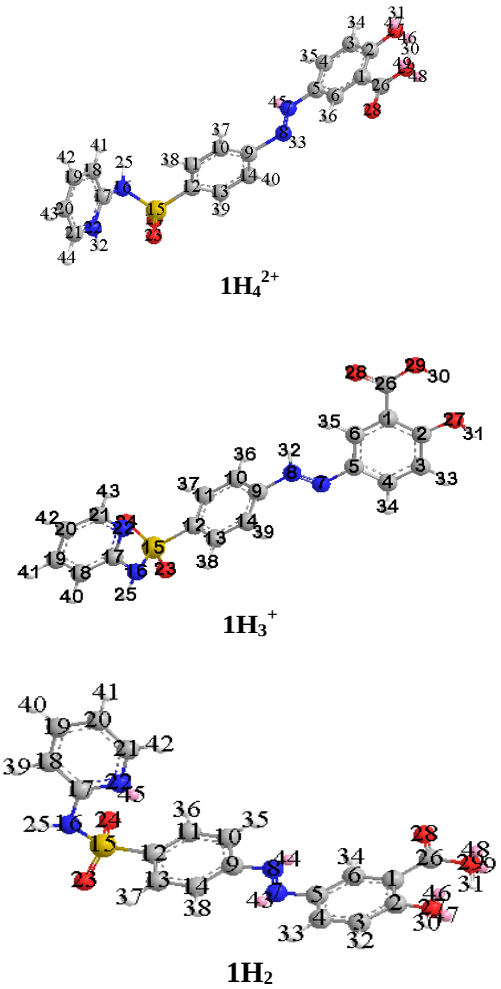

Figure 8: ***Stereographic ball and stick***

Molecular Modeling

Molecular modeling studies were carried out on **1H$_2$** using Cambridge Soft Chem Office Ultra software. The calculated thermodynamic values of various acid-base conjugate species in several of their tautomeric forms are collected in **Table 3.** The global energy-minimized structure of the most thermodynamically stable species of **1H$_2$** is shown in **Figure 8** in its stereographic projection along with the numbering scheme for the atoms. Conformational double-dihedral drive energy trends of **1H$_4^{2+}$**, **1H$_3^+$**, **1H$_2$**, **1H$^-$** and **1^{2-}** over C(12)-S(15)-N(16) bonds have been used (**Figure 9**) to finalize the most stable conformers of **1H$_2$** and its acid-base conjugates for finalizing their most stable acid-base conjugates, viz., **1H$_4^{2+}$**, **1H$_3^+$(N$_{sul}$)**, **1H$_2$(ZwtPh)**, **1H$^-$(Carb)** and **1^{2-}(Quin)**,

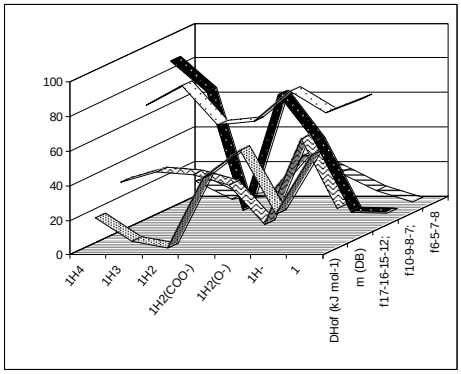

Figure 9: *Conformational double-dihedral drive energy trends of* $1H_4^{2+}$, $1H_3^{+}$, $1H_2$, $1H^{-}$ *and* 1^{2-} *over C(12)-S(15)-N(16)* bonds

The quantum mechanical HOMO-LUMO energy calculations have been used for computing the expected gas-phase electronic transitions for various conjugates and tautomers of **$1H_2$**. These values are also collected in **Table 3** along with the experimental spectral data. The trends of the theoretical and experimental absorption maxima are in good agreement.

Table 1: ***Spectral and thermodynamic data of*** $^{\#}$ ***$1H_2$.***

Colour	MP	Solubility	$\lambda_{low}(\varepsilon)$	$\lambda_{high}(\varepsilon)$	$\lambda_{iso}(\varepsilon)$	pK_a	pK_b	K_a x10^{11}	ΔG^o
Yellow	240-245	Ethanol, NaOH	355.5 ($9.24x10^3$)	455.2 ($1.11x10^4$)	388.2 ($5.71x10^3$)	10.83	3.17	1.479	5.71

λ in nm; ε (in lt mol-1 cm^{-1}); K_a and ΔG^o (in kJ mol^{-1}) are for the process. λ_{low} and λ_{high} are wave lengths below and above the isobestic wave length, λ_{iso}, respectively.

Table 2- ***Voltammetric data of $1H_2$.***

pH	**$-E_p$** (V) vs Ag|AgCl	**i_p** (μA)	**αn_a**	**D_o** x 10^6 (cm^2 s^{-1})	**$k^o_{f,h}$** x10^9 (cm^2 s^{-1})
2.42	0.113	0.625	0.61	3.14	5.37
4.32	0.202	0.158	0.70	1.75	7.07
6.1	0.381	0.21	0.67	3.25	3.49
8.65	0.595	0.084	0.41	8.51	3.96
10.25	0.763	0.0383	0.73	9.83	6.49
11.5	0.859	0.0472	1.64	6.71	8.31

Table 3: Molecular modeling data of various stable conjugate species of $1H_2$.

Property/ Species	$1H_4^{2+}$	$1H_3^+$			$1H_2$			$1H^-$		1^{2-}	
		N_{Pyr}	N_{Sul}	N_{Sal}	**Neut**	**ZwtPh**	**ZwtCa**	**Phen**	**Carb**	**Benz**	**Quin**
ΔH^o_f(kJ mol^{-1})	**17.69**	**-4.01**	**-6.39**	-4.76	-2.64	-59.16	-18.00	-19.10	-22.76	-18.79	-54.52
Dihedrals											
$\phi_{15\text{-}16\text{-}17\text{-}18}$	49.80	29.30	39.50	45.80	19.80	39.40	38.90	29.30	29.50	29.30	12.60
$\phi_{12\text{-}15\text{-}16\text{-}17}$	70.10	30.70	64.40	87.90	54.10	60.00	57.80	59.90	60.00	59.90	68.60
$\phi_{11\text{-}12\text{-}15\text{-}16}$	30.10	32.70	36.90	2.00	45.30	49.10	49.80	41.30	42.30	42.20	3.40
$\phi_{7\text{-}8\text{-}9\text{-}10}$	90.00	0.60	90.80	19.30	0.10	58.80	57.70	0.40	0.40	0.50	2.50
$\phi_{5\text{-}7\text{-}8\text{-}9}$	4.60	0.20	0.70	1.70	0.20	0.30	0.20	0.70	0.60	0.50	1.90
$\phi_{4\text{-}5\text{-}7\text{-}8}$	17.60	0.10	0.00	88.70	0.30	15.90	14.80	0.20	0.10	0.20	2.30
HOMO	-1.675		-2.008		-3.950	-3.520	-5.330	-6.702		-4.792	
LUMO	-3.757		-3.770		-4.793	-8.978	-8.376	-8.418		-9.711	
(LUMO-HOMO)	2.08		1.76		0.84	5.46	3.05	1.72		4.92	
λ_{max}^*	571.9		675.7		1412.3	218.1	390.9	693.8		242.0	

REFERENCES

1. Garg HG, Sharma RA. J Med Chem, 1996; 12: 1122.
2. Ravindranath LK, Ramadas SR, Rao SB, Electrochim Acta, 1983; 28: 601.
3. Suneel Kumar M. PhD Thesis, Spectral, Electrochemical and Photochemical studies and molecular modeling of Azobenzene and Stilbene Derivatives, NIT Warangal, 1999.
4. Kelemen J, Dyes Pigments, 1982; 2: 73.
5. Çakır O, Biçer E, Portugaliae Electrochimica Acta, 1998; 16: 11.
6. Malik WU, Goyal RN, Jain R, J Electroanal Chem, 1978; 87: 129.
7. Malik WU, Goyal RN, Talanta, 1976; 23: 705.
8. Xu G, O'Dea JJ, Osteryoung JG, Dyes Pigments, 1996; 30: 201.
9. Ju Luirie, Handbook of Analytical Chemistry, Mir Publishers Moscow, 1978.
10. Hillson PJ, Birnbaum PP, Trans Faraday SOC, 1952; 48: 478.
11. Castor CR, SaylorJH, J Am Chem Soc, 1953; 75: 1427.
12. Wawzonek S, Fredrickson JD, J Am Chem Soc, 1955; 77: 3985.
13. Markman AL, Zinkova EV J Gen Chem USSR, 1959 ; 29: 3058.
14. Laviron E, Mugnier Y, J Elecrroanal Chem 1980; 111: 337.
15. Oglesby DM, Johnson JD, Reilley CN, Anal Chem, 1966; 38: 385.
16. Saul Patai, The chemistry of the Hydrazo, Azo and Azoxy Groups, Part-1, John Wiley & Sons: New York, 1975: 443.